A Theoretical Study of Complexes MH_x^{2-} and MCl_y^{2-} in Crystalline A_2MH_x and A_2MCl_y Compounds (A = Alkali, Alkaline Earth; M = Ni, Pd, Pt; x = 2, 4, 6; y = 4, 6)

Meng-sheng Liao* and Qian-er Zhang

Department of Chemistry, State Key Laboratory for Physical Chemistry of Solid Surfaces, Xiamen University, Xiamen, Fujian 361005, P.R. China

Received April 4, 1996[⊗]

A theoretical study of the complexes MH_x^{2-} and MCl_y^{2-} in the crystalline A_2MH_x and A_2MCl_y compounds (A = alkali, alkaline earth; M = Ni, Pd, Pt; x = 2, 4, 6; y = 4, 6) has been carried out using a relativistic density-functional method. A cutoff-type Madelung potential (MP) was used to take into account the crystalline environment. Energies, geometries, force constants, and vibrational frequencies have been determined. The relative stability of ML_6^{2-} versus ML_4^{2-} has been evaluated by the decomposition reaction of $ML_6^{2-} \rightarrow ML_4^{2-} + L_2(g)$ (L = H, Cl). The experimental M−H and M−Cl distances and their trends within the group 10 elements are very well reproduced by the calculations in the MP. The long-range electrostatic potential and the short-range repulsion between Na^+ and its trans neighboring Na^+ ions are responsible for the especially long H−Na bond length in the Na_2PdH_2 compound. All free ML_6^{2-} complexes are predicted to be rather stable against disproportionation. The crystal field effect strongly shifts the equilibrium to the right. The calculated reaction energies in the MP reveal that, in the solid state, $PdCl_6^{2-}$ and $PtCl_6^{2-}$ are stable but NiH_6^{2-}, PdH_6^{2-}, and $NiCl_6^{2-}$ are rather unstable. The results are in agreement with the experimental evidence and also confirm the fact that the phenomenon of higher valency in compounds depends on the metal (M) and the choice of ligand (L). The relativistic effects strongly support the higher oxidation state in the metals.

1. Introduction

The ternary hydrides A_zMH_x in which A is an alkali or alkaline-earth metal and M is a transition metal, form interesting solid compounds[1] that have a range of properties varying from metallic to saltlike. A striking feature of the structures is the presence of isolated $[MH_x]$ complexes in all so far determined crystal structures, where the hydrogens are rather strongly bound to the transition metal. Another special feature is the dynamic behavior of the hydrogen ligands; i.e., atomic arrangements in some hydrides with $x < 6$ at high temperature (HT) are different from those at low temperature (LT). In the HT phase, the hydrogen has a high local mobility, so that the hydrogen atoms are distributed in a statistical manner and an octahedron around the M atom is observed on the average; in the LT phase, this movement of the hydrogen atoms is frozen and the basic motion is a vibratory one. The third feature is that many A_zMH_x hydrides show great structural similarities to the corresponding chlorides K_2MCl_y (M = Pd, Pt; y = 4, 6).[2−6]

The aim of this paper is to give a theoretical investigation of bonding properties of the complexes $[MH_x]$ in the crystalline A_zMH_x compounds. So far, only a few A_zMH_x solids have been experimentally studied in detail, and those that are known at present nearly all belong to groups 8, 9, and 10 (i.e., subgroup 8) of the periodic table. In order to restrict the general discussion, the present paper only deals with compounds involving group 10 elements. Compounds of this group usually have the formula A_2MH_x with x = 2, 4, or 6. If the conventional charge of 1+ is assumed for the alkali, the transition metal hydrogen complex receives a charge of 2−, forming MH_x^{2-} in the crystals.

The PdH_2^{2-} groups are contained in Li_2PdH_2[7] and Na_2PdH_2.[8] The stoichiometric composition results in an oxidation number of zero for Pd and thus the ligand coordination is linear and corresponds to that in analogous Ag(I) complexes. Corresponding linear PtH_2^{2-} units were found in a mixed-crystal system Na/Pd/Pt/H[9a] as well as in Li_2PtH_2.[9b] The PdH_4^{2-} groups are contained in Na_2PdH_4[10] and K_2PdH_4.[11] The PdH_4^{2-} units were also found to exist in the host of Na_2PtH_4.[9a] There are a series of alkali platinum hydrides that contain the isolated PtH_4^{2-} groups (A = Na, K, Rb, Cs).[12−16] The four H ligands attached to the metal atom with its d^8 configuration result in the expected planar square coordination. The $[NiH_4]$ complexes are found only in the Mg_2NiH_4 crystal.[17−19] If the conventional charge of 2+ is assumed for Mg, the $[NiH_4]$ complex then receives a

* Corresponding author.

[⊗] Abstract published in *Advance ACS Abstracts,* January 1, 1997.

(1) Bronger, W. *Angew. Chem., Int. Ed. Engl.* **1991**, *30*, 759.
(2) Dickinson, R. G. *J. Am. Chem. Soc.* **1922**, *44*, 2404.
(3) Mais, R. H. B.; Owston, P. G.; Wood, A. M. *Acta Crystallogr.* **1972**, *B28*, 393.
(4) Ohba, S.; Sato, S.; Saito, Y. *Acta Crystallogr.* **1983**, *B39*, 49.
(5) Ohba, S.; Saito, Y. *Acta Crystallogr.* **1984**, *C40*, 1639.
(6) Takazawa, H.; Ohba, S.; Saito, Y. *Acta Crystallogr.* **1988**, *B44*, 580.
(7) Kadir, K.; Noreus, D. *Z. Phys. Chem. N.F.* **1989**, *163*, 231.
(8) Noreus, D.; Törnroos, K. W.; Börje, A.; Szabo, T.; Bronger, W.; Spittank, H.; Auffermann, G.; Müller, P. *J. Less-Common Met.* **1988**, *139*, 233.
(9) (a) Bronger, W.; Auffermann, G. *J. Less-Common Met.* **1991**, *169*, 173. (b) Bronger, W.; á Brassard, L. *Z. Anorg. Allg. Chem.* **1996**, *622*, 462.
(10) Bronger, W.; Auffermann, G. *J. Alloys Compd.* **1995**, *228*, 119.
(11) Kadir, K.; Kritikos, M.; Noréus, D.; Andresen, A. F. *J. Less-Common Met.* **1991**, *172*, 36.
(12) Bronger, W.; Müller, P.; Schmitz, D.; Spittank, H. *Z. Anorg. Allg. Chem.* **1984**, *516*, 35.
(13) Bronger, W.; Auffermann, G.; Hofmann, K.; Müller, P. *Z. Kristallogr.* **1985**, *170*, 37.
(14) Bronger, W.; Auffermann, G.; Müller, P. *J. Less-Common Met.* **1986**, *116*, 9.
(15) Bronger, W.; Auffermann, G.; Müller, P. *Z. Kristallogr.* **1987**, *178*, 37.
(16) Bronger, W.; Auffermann, G.; Müller, P. *J. Less-Common Met.* **1988**, *142*, 243.
(17) Yvon, K.; Schefer, J.; Stucki, F. *Inorg. Chem.* **1981**, *20*, 2776.
(18) Noreus, D.; Olsson, L. G. *J. Chem. Phys.* **1983**, *78*, 2419.
(19) Zolliker, P.; Yvon, K.; Jorgensen, J. D.; Rotella, F. J. *Inorg. Chem.* **1986**, *25*, 3590.

S0020-1669(96)00369-2 CCC: $14.00

charge of 4−. The most possible configuration should be tetrahedral for Ni^0. However, a neutron scattering study[18] and an infrared (IR) investigation[20] at HT favor a planar square arrangement of the [NiH_4] complex, similar to the situation in A_2PtH_4. Mg_2NiH_4 has already attracted some special interest in connection with application as a hydrogen storage medium. The first theoretical study of the local H atom configurations was carried out by Lindberg et al.[21] using CASSCF and CI methods. The more accurate CI calculation was used to explain the configuration of a NiH_4^{n-} complex as a function of its charge *n*. A more recent theoretical study was carried out by Huang et al.[20,22] from the viewpoint of entropy. There were also some band structure calculations on Na_2PdH_2[23] and K_2PdH_4[24] within the muffin tin approximation.

The presence of the MH_6^{2-} groups in crystalline A_2MH_x compounds had not been established until very recently,[25−27] but the compounds were prepared only under very high H_2 pressure (1500−1800 bar). On the other hand, the transition metal that has been found to reach the higher oxidation state IV seems to be limited only to platinum within group 10 hydrides. The reaction of sodium hydrides with palladium yielded only Na_2PdH_4 by using a method analogous to that for synthesizing Na_2PtH_6. This is in contrast to the chlorides, where the $PdCl_6^{2-}$ groups in crystalline compounds were well characterized.[6] Therefore the question of whether the palladium could be oxidized beyond the oxidation state II still remains. In the discussion of the bonding properties of the hydrides, it is interesting to include chlorides with isotypic or closely related structures K_2MCl_y (M = Pd, Pt; $y = 4, 6$) in our calculations. In fact, the interpretation of the physical and chemical properties of the $PdCl_4^{2-}$ and $PtCl_4^{2-}$ complexes has been the subject of experimental[28−30] and theoretical[31−34] interest. The first calculation of an ab initio nature was carried out by Messmer et al.[33] using a self-consistent-field X_α-scattered wave (SCF-X_α-SW) method. Later, a relativistic calculation of the complexes was carried out by Larsson and Olsson[34] using the Dirac−Slater method. However, the previous theoretical studies concentrated mainly on the assignment of electronic spectra. There has been no emphasis on an evaluation of the M−Cl bond strengths. On the other hand, these theoretical studies were only devoted to the free complexes. Our main interest here focuses on the bond lengths, bond energies, and force constants. The effects of both relativity and crystal field on the complexes are considered. The relative stability of M(IV) versus M(II) in the hydrides will be discussed and compared to that in the chlorides. For the sake of comparison, our calculations include several hypothetical crystals.

2. Calculation Details

2.1. Calculational Method and Basis Sets. All calculations were carried out by using the relativistic Amsterdam density-functional (ADF) program system.[35] The ADF method uses the expansion of the one-electron molecular functions in atomic-centered STO basis sets. The specified core electrons are described in the frozen core approximation.[35b] The relativistic corrections of the valence electrons are calculated by first-order perturbation method,[36] which is based on the Foldy−Wouthuysen transformation of the Dirac−Fock equation. Its Hamiltonian contains mass velocity, Darwin, "indirect effect", and spin−orbit corrections. The inner atomic core orbitals are calculated by the Hartree− and Dirac−Fock−Slater methods. The so-called "indirect effect" is caused by the relativistic change of core potential.

In the present work, the exchange correlation potential of Vosko, Wilk, and Nusair (VWN)[37] plus Stoll's dynamical correction[38] to the correlation energy was used throughout the calculations. The STO basis used is of triple-ζ quality for all atoms and relatively small core definitions ([Ne] for Ni, [Ar3d^{10}] for Pd, [Kr4d^{10}4f^{14}] for Pt) are used for the transition metals; the valence set on the transition metals includes $(n-1)$s and $(n-1)$p shells. Besides, we add two polarization functions of the *n*p type for the transition metals. For the light atoms Cl and H we add one polarization function of the 3d and 2p types, respectively. On Cl, the core has been kept frozen until 2p.

2.2. Crystal Structures. The following real crystal structures were employed: Na_2PdH_2,[8] Mg_2NiH_4,[17] K_2PdH_4,[11] K_2PtH_4,[16] K_2PtH_6,[25] K_2PdCl_4,[6] K_2PtCl_4,[4] K_2PdCl_6,[6] and K_2PtCl_6.[5] Because the crystal structure type of Li_2PtH_2[9b] is somewhat different from that of Na_2PdH_2, the Li_2PtH_2 compound has not been included in the present calculations. In fact, there are a series of questions involved in Li_2PtH_2, for which we will give a detailed discussion in a separate paper. All crystallographic data of the above compounds are given in Table 1. As already pointed out, the hydrides have crystal structures containing isolated MH_x^{2-} ($x = 2, 4, 6$) complexes and the crystal structures of the chlorides contain isolated MCl_y^{2-} ($y = 4, 6$) complexes. Here the numbers 2, 4, and 6 also indicate that the geometries of the complexes are linear, square, and octahedral, respectively. Both Mg_2NiH_4 and K_2PtH_4 possess LT and HT phases. Their HT phase corresponds to the K_2PtCl_6 structure type (see Figure 1) with H occupying two-thirds of the Cl positions. Here only the HT phase structures are chosen in the calculations. K_2PdH_4 crystallizes in a new structure type (see Figure 2), but it shows great similarity to the K_2PtCl_4 structure type (Figure 3). The difference between K_2PtCl_4 and K_2PdH_4 is that the $PtCl_4^{2-}$ groups are stacked in the $\vec{c}$ direction with interaction between the $PtCl_4^{2-}$ groups in one dimension, while the PdH_4^{2-} groups are stacked alternately in the $\vec{c}$ direction. The atomic arrangement in K_2PtH_6 was shown[25] to be isotypic with that of K_2PtCl_6; i.e., the six octahedral sites around the platinum in the cubic K_2PtH_4 are now fully occupied. Besides, the size of the unit cell of this hydrogen-enriched phase is quite similar to that of K_2PtH_4. Because of the lack of possibility for the mobility of the hydrogen atoms within the PtH_6^{2-} group, the phase

(20) Huang, N.; Yamauchi, H.; Wu, J.; Wang, Q.-D. *Z. Phys. Chem. N.F.* **1989**, *163*, 225.
(21) Lindberg, P.; Noreus, D.; Blomberg, M. R. A.; Siegbahn, P. E. M. *J. Chem. Phys.* **1986**, *85*, 4530.
(22) Huang, N.; Wang, Q.-D.; Wu, J.; Tang, J.-C. *Z. Phys. Chem. N.F.* **1989**, *163*, 207.
(23) Gupta, M.; Temmermann, W. M. *J. Phys.: Condens. Matter* **1991**, *3*, 871.
(24) (a) Gupta, M. *Z. Phys. Chem.* **1993**, *181*, 9. (b) Switendick, A. C. *Z. Phys. Chem.* **1993**, *181*, 19.
(25) Bronger, W.; Auffermann, G. *Angew. Chem., Int. Ed. Engl.* **1994**, *33*, 1112.
(26) Bronger, W.; Auffermann, G. *J. Alloys Compd.* **1995**, *219*, 45.
(27) Bronger, W.; Auffermann, G. *Z. Anorg. Allg. Chem.* **1995**, *621*, 1318.
(28) Chatt, J.; Gamlen, G. A.; Orgel, L. E. *J. Chem. Soc.* **1958**, 486.
(29) Anex, B. G.; Takeuchi, N. *J. Am. Chem. Soc.* **1974**, *96*, 4411.
(30) Elding, L. I.; Olsson, L.-F. *J. Phys. Chem.* **1978**, *82*, 69.
(31) Fenske, R. F.; Martin, J. R., D. S.; Ruedenberg, K. *Inorg. Chem.* **1962**, *1*, 441.
(32) Gray, B. H.; Ballhausen, C. J. *J. Am. Chem. Soc.* **1963**, *85*, 260.
(33) Messmer, R. P.; Interrante, L. V.; Johnson, K. H. *J. Am. Chem. Soc.* **1974**, *96*, 3847.
(34) Larsson, S.; Olsson, L.-F. *Int. J. Quant. Chem.* **1984**, *25*, 201.
(35) (a) Baerends, E. J. *ADF program package: Version 1989*; Free University: Amsterdam, 1989. (b) Baerends, E. J.; Ellis, D. E.; Ros, P. *Chem. Phys.* **1973**, *2*, 41. (c) te Velde, G.; Baerends, E. J. *J. Comput. Phys.* **1992**, *99*, 84.
(36) (a) Snijders, J. G.; Baerends, E. J. *Mol. Phys.* **1978**, *36*, 1789. (b) Snijders, J. G.; Baerends, E. J. *Mol. Phys.* **1979**, *38*, 1909. (c) Ziegler, T.; Snijders, J. G.; Baerends, E. J. *J. Chem. Phys.* **1981**, *74*, 1271.
(37) Vosko, S. H.; Wilk, L.; Nusair, M. *Can. J. Phys.* **1980**, *58*, 1200.
(38) Stoll, H.; Pavlidou, C. M. E.; Preuss, H. *Theor. Chim. Acta* **1978**, *149*, 143.

Table 1. Crystal Structure Data and Nearest Interatomic Distances

compds	crystal structure data[a]	nearest interatomic distances[b] (Å)
Na_2PdH_2	tetragonal, I_4/mmm, $Z = 2$, $a = b = 3.596$, $c = 11.308$	Pd−H = 1.64(2×), Pd−Na = 3.00(4×), Pd−Pd = 3.60(4×), H−Na[c] = 2.54(4×), H−H = 3.28(4×), Na−Na[c] = 3.55(4×)
Mg_2NiH_4	cubic, $Fm3m$, $Z = 4$ $a = b = c = 6.507$	Ni−H = 1.49(4×), Ni−Mg = 2.82(8×), Ni−Ni = 4.60(12×), H−Mg = 2.31(4×), H−H[c] = 2.49(4×), Mg−Mg = 3.25(6×)
K_2PdH_4	tetragonal, I_4/mmm, $Z = 2$, $a = b = 5.831$, $c = 7.692$	H−K = 2.85(4×), H−H[c] = 3.94(2×), K−K = 3.85(2×)
K_2PtH_4	cubic, $Fm3m$, $Z = 4$, $a = b = c = 8.025$	Pt−H = 1.62(4×), Pt−K = 3.48(8×), Pt−Pt = 5.68(12×), H−K = 2.86(4×), H−H[c] = 3.38(4×), K−K = 4.01(6×)
K_2PtH_6	cubic, $Fm3m$, $Z = 4$, $a = b = c = 8.176$	Pt−H = 1.65(6×), Pt−K = 3.54(8×), Pt−Pt = 5.78(12×), H−K = 2.92(4×), H−H[c] = 3.45(4×), K−K = 4.09(6×)
K_2PdCl_4	tetragonal, P_4/mmm, $Z = 1$, $a = b = 7.026$, $c = 4.080$	Pd−Cl = 2.29(4×), Pd−K = 4.06(8×), Pd−Pd = 4.08(2×), Cl−K = 3.22(4×), Cl−Cl[c] = 3.79(2×), K−K = 4.08(2×)
K_2PtCl_4	tetragonal, P_4/mmm, $Z = 1$, $a = b = 7.024$, $c = 4.147$	Pt−Cl = 2.31(4×), Pt−K = 4.08(8×), Pt−Pt = 4.15(2×), Cl−K = 3.24(4×), Cl−Cl[c] = 3.76(2×), K−K = 4.15(2×)
K_2PdCl_6	cubic, $Fm3m$, $Z = 4$ $a = b = c = 9.637$	Pd−Cl = 2.29(6×), Pd−K = 4.17(8×), Pd−Pd = 6.82(12×), Cl−K = 3.41(4×), Cl−Cl[c] = 3.57(4×), K−K = 4.82(6×)
K_2PtCl_6	cubic, $Fm3m$, $Z = 4$ $a = b = c = 9.743$	similar to those in K_2PdCl_6
K_2NiCl_4 (hypoth)	tetragonal, P_4/mmm, $Z = 1$, $a = b = 6.842$, $c = 3.840$	Ni−Cl = 2.16(4×)
K_2NiCl_6 (hypoth)	cubic, $Fm3m$, $Z = 4$ $a = b = c = 9.117$	Ni−Cl = 2.16(6×)

[a] Lattice constants are in angstroms. [b] Coordination numbers are in parentheses. [c] Second nearest interatomic distance between two atoms of neighboring molecules.

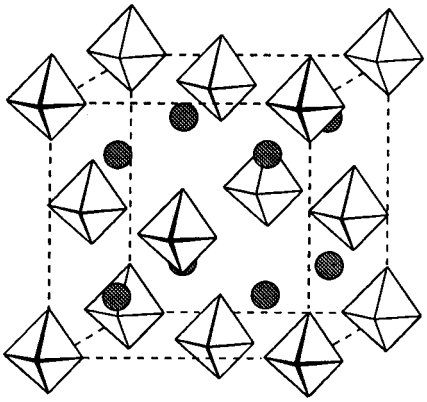

Figure 1. Crystal structure of the $K_2[PtCl_6]$ type, showing the positions of the M−L octahedron.

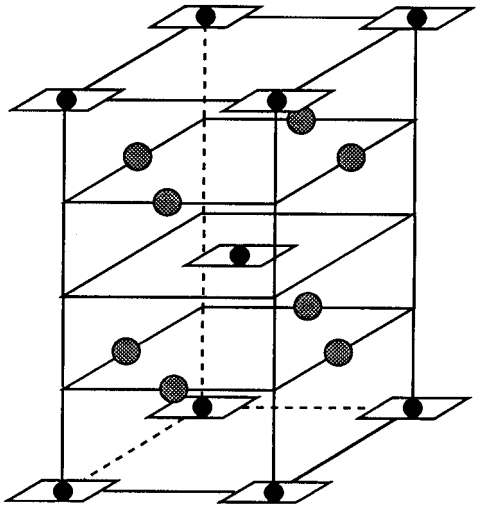

Figure 2. Crystal structure of $K_2[PdH_4]$. The small dark balls represent the Pd atom.

transition (HT phase → LT phase) for K_2PtH_6 does not happen any longer. The unit cell of the Na_2PdH_2 crystal is shown in Figure 4. There is no known chloride crystal structure corresponding to this, but Na_2PdH_2 is isotypic with the oxide Na_2HgO_2[39] where the central atom has the a same d^{10} configuration.

(39) Hoppe, R.; Röhrborn, H. J. *Z. Anorg. Allg. Chem.* **1964**, *329*, 110.

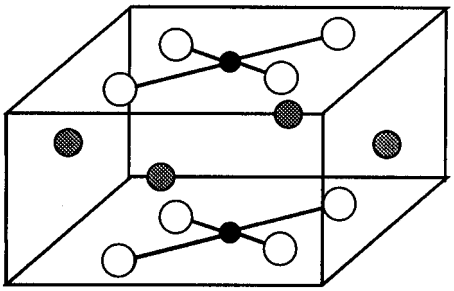

Figure 3. Crystal structure of the $K_2[PtCl_4]$ type. The small dark balls represent the transition atom.

The linear PdH_2^{2-} group is oriented along (001). In $\vec{c}$-direction, there is close approach of 2.42 Å between H and Na. So the linear Na_2PdH_2 group can be considered to form a typical building block of the structure. In practice, the two nearest-neighbors Na are explicitly included in the calculation, and so the calculated moiety corresponds to the formula of the compound. The K_2PdCl_4 and K_2PtCl_4 crystal structures are equivalent and so are K_2PdCl_6 and K_2PtCl_6.

No corresponding crystal compounds A_2PdH_6, Na_2PtH_2, and A_2NiCl_y ($y = 4$, 6) are known experimentally. In order to explore and predict the trends within the hydride and chloride groups, hypothetical crystal compounds K_2PdH_6, Na_2PtH_2, and K_2NiCl_y were used in the calculations. We assumed the crystal structures of Na_2PdH_2, K_2PtH_6, and K_2PdCl_y for Na_2PtH_2, K_2PdH_6, and K_2NiCl_y, respectively. Since Pd and Pt are of nearly same size, the lattice constants of A_2PdH_x and A_2PtH_x are also assumed to be same. The lattice constants for K_2NiCl_y have to be scaled appropriately. In K_2PdCl_4, the Pd and K atoms lie on special positions in the tetragonal lattice (see Figure 3). The nearest interatomic Pd−Pd distance represents the lattice constant c. The $\vec{a}$ direction contains two Pd−Cl entities in a unit cell. The lattice constants a and b for an isostructural crystal K_2MCl_4 are expressed as

$$a = b = 2R_{MCl}\sin(\pi/4) + R(Cl\cdots Cl) \qquad (1)$$

The atomic radii of Ni is 0.13 Å smaller than that of Pd. So the lattice constant c of the hypothetical K_2NiCl_4 crystal is 0.26 Å less than that of K_2PdCl_4. In eq 1 the M−Cl bond length is the only variable parameter. According to calculated results

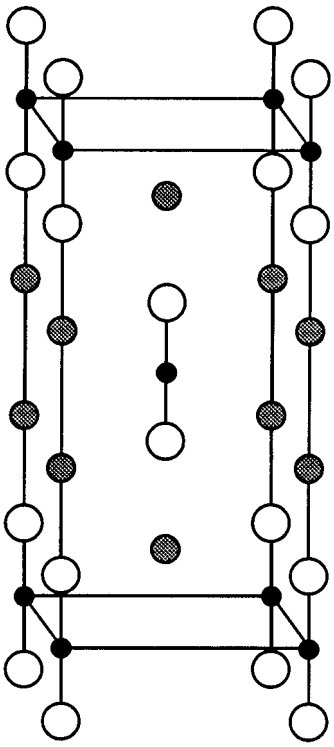

Figure 4. Crystal structure of the $Na_2[PdH_2]$. The small dark balls represent the Pd atom.

of free MCl_4^{2-} complexes (see section 3.2), the Ni−Cl bond length is 0.12 Å shorter than the Pd−Cl bond length. We suppose that the difference between R_{PdCl}^{free} and R_{NiCl}^{free} extends to the solid compounds. In K_2PdCl_6, each direction in one unit cell contains four Pd−Cl entities (see Figure 1). Therefore, the lattice constants of K_2NiCl_6 are calculated as

$$a = b = c = 4R_{NiCl} + \Delta \tag{2}$$

where $\Delta = a(K_2PdCl_6) - 4R_{PdCl}$. All the obtained lattice constants are also given in Table 1.

In calculating the hypothetical NiH_6^{2-} complexes in the crystal structure, the corresponding Mg_2NiH_4 crystal structures (HT phase) were used.

2.3. Crystal Fields. According the atomic arrangements in these (ionic) compounds, there is a quite large metal−metal separation (see Table 1), and so the interaction between units can be considered to be small. We may assume that the predominant effects on the complex properties can be attributed to the electrostatic interaction from the surroundings. As a simple model, the surrounding atoms are treated as a set of infinite point charges that create a Madelung potential (MP) in which the complex ion is immersed. The so-called point charge model have been successful in studying many solid-state compounds.[40,41] In calculating the Madelung potentials, the formal charge of 1− is assumed for H and Cl. In view of the fact that H atoms are mainly in square-planar configurations around the Ni atoms in Mg_2NiH_4, a formal charge of 1+ is here considered on the Mg atom, yielding the NiH_4^{2-} complex. The Madelung potentials are evaluated through the Ewald method.[42] The outcome of the calculation is the value of the potential in a number of grid points in the molecular region. Then a certain number (40−100) of point charges at the lattice sites are put around it, the charge of which is determined by a least-squares fit to the calculated potential in the grid points.

The simple point charge model can only take into account the long-range electrostatic interaction but neglects the short-range overlap from the nearest neighbors. A slight modification for the Madelung potential has been made by using a Coulomb cutoff-type pseudopotential

$$V_{effective}(r) = \max(V_{Madelung}(r), C) \tag{3}$$

It accounts for the fact that the valence electrons of the ion group must not penetrate into the electrostatically attractive core regions of the surrounding anions or cations because of the Pauli exclusion repulsion. C is a constant used in cutoff-type effective core potentials[43] to balance the nuclear attraction.

Along the point charge model, the bond energy now consists of two parts

$$E_{bond}^{total} = \frac{1}{2}E_{latt} + E_{bond}^{internal} \tag{4}$$

where $E_{bond}^{internal}$ is the bond energy of the complex, as calculated in the crystal field. E_{latt} is the electrostatic interaction between the complex fragments and the lattice

$$E_{latt} = \sum_A [\int \rho_A(\vec{r})\mathrm{MP}(\vec{r})\, \mathrm{d}\vec{r} + Z_A\mathrm{MP}(R_A)] \tag{5}$$

3. Results and Discussion

The results (bond lengths, bond energies, force constants, vibrational frequencies) for Na_2MH_2 (M = Pd, Pt) are given in Table 2. The linear symmetric Na−H−M−H−Na molecule contains two types of bonds r_1 (M−H) and r_2 (H−Na). We have optimized r_1 and r_2 simultaneously. First the potential energy of the system is expressed in terms of the changes of the bond lengths r_1 and r_2 with the most general quadratic polynomial

$$E(r_1,r_2) = \beta_1 r_1^{\,2} + \beta_2 r_2^{\,2} + \beta_3 r_1 r_2 + \beta_4 r_1 + \beta_5 r_2 + \beta_6 \tag{6}$$

A number of calculated energy points around the equilibrium were adopted to fit this model. We then gave an estimate of the six independent constants β_1, β_2, ..., β_6 which satisfy the least-squares criterion. From this the equilibrium distances, R_1 and R_2, and bond energy, E_{bond}, are obtained. This also leads to a relation between the parameters β_1, β_2, and β_3 and the force constants k_1, k_2, and k_{12}: $k_1 = \beta_1$, $k_2 = \beta_2$, and $k_{12} = \beta_3/2$, where k_1 represents bond stretching of M−H, k_2 represents that of H−Na, and k_{12} corresponds to the interaction between adjacent bonds r_1 and r_2. We can then set up the secular equation to determine the frequencies, ω. For the linear molecules, three normal parallel vibrational frequencies have been determined, ω_1 [Σ_g, (H···H)], ω_2 [Σ_u, (H−Na)], and ω_3 [Σ_g, (H−Na)]. The form of the vibrations ω_1, ω_2, and ω_3 is shown in Figure 5. ω_1 is essentially a H···H vibration and ω_3 is a H−Na vibration.

The M−H bond energy in Na_2MH_2 is defined as

$$E_{MH} = -\frac{1}{2}\{E(Na_2MH_2) - E(M) - 2E(HNa)\} \tag{7}$$

where $E(Na_2MH_2)$ is the total energy of the molecule Na_2MH_2, $E(M)$ the total energy of M, and $E(HNa)$ the total energy of

(40) Liao, M.-S.; Zhang, Q.-E.; Schwarz, W. H. E. *Inorg. Chem.* **1995**, *34*, 5597.
(41) Liao, M.-S.; Schwarz, W. H. E. *J. Alloy Compd.*, in press.
(42) Ewald, P. P. *Ann. Phys.* **1921**, *64*, 253.
(43) Kutzelnigg, W.; Koch, R. J.; Bingel, W. A. *Chem. Phys. Lett.* **1968**, *2*, 197.

Table 2. Calculated Bond Lengths R (Å), Bond Energie E_{MH} (eV), Lattice Energies E_{latt} (eV), Force Constants k (mdyn/Å), and frequencies ω (cm^{-1}) in MH_2^{2-} and Na_2MH_2[a]

	R_{MH}			R_{NaH}		
	FM(I)	MMP	exp	FM	MMP	exp
PdH_2^{2-}	1.68 (1.71)					
PtH_2^{2-}	1.70 (1.78)					
Na_2PdH_2	1.62 (1.65)	1.66 (1.69) 1.67[c]	1.64	1.90 (1.87)	2.17 (2.09) 2.40[c]	2.42
Na_2PtH_2	1.62 (1.70)	1.68 (1.75)		1.88 (1.86)	2.21 (2.10)	

	FM(I)		MMP			
	E_{MH}	Δ^{rel}	$E_{MH}^{internal}$	$(^1/_2E_{latt})^b/2$	E_{MH}^{total}	Δ^{rel}
PdH_2^{2-}	1.32 (0.94)	0.38				
PtH_2^{2-}	1.50 (0.73)	0.77				
Na_2PdH_2	2.28 (1.88)	0.40	4.73 (4.00)	0.55 (0.53)	5.28 (4.53)	0.75
Na_2PtH_2	2.62 (1.86)	0.76	5.28 (4.03)	0.48 (0.47)	5.76 (4.50)	1.26

	k_{MH}			k_{NaH}		k_{12}	
	FM(I)	MMP	exp	FM	MMP	FM	MMP
PdH_2^{2-}	1.70 (1.46)						
PtH_2^{2-}	1.88 (1.33)						
Na_2PdH_2	2.18 (1.82)	2.22 (1.84)	1.98	0.65 (0.69)	0.25 (0.48)	−0.06 (−0.04)	0.00 (0.18)
Na_2PtH_2	2.38 (1.92)	2.52 (1.74)		0.66 (0.71)	0.33 (0.33)	−0.06 (−0.04)	0.16 (0.04)

	ω_1		ω_2		ω_3	
	FM(I)	MMP	FM	MMP	FM	MMP
PdH_2^{2-}	1697 (1573)					
PtH_2^{2-}	1785 (1501)					
Na_2PdH_2	188 (189)	130 (179)	1072 (1103)	669 (925)	2230 (2092)	2046 (1826)
Na_2PtH_2	191 (191)	154 (144)	1081 (1118)	766 (758)	2313 (2145)	2067 (1843)

[a] The values in parentheses are the nonrelativistic results. FM(I), freem molecule (or ion); MMP, molecule in Madelung potential. [b] The relativistic and nonrelativistic E_{latt}'s represent lattice energies calculated at R^{rel} and R^{nrel}, respectively. [c] Calculated in eight alkali ligands A^+ and crystal field surrounding.

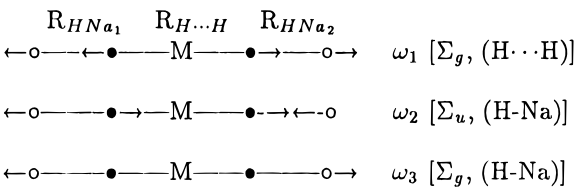

Figure 5. Longitudinal vibrations of Na_2MH_2. (●) H; (○) Na.

HNa (the H−Na distance of the free HNa fragment is independently optimized).

The results of the ML_n^{2-} (L = H, Cl) complexes are collected in Tables 3 and 4. The optimization of the M−L bond length has been carried out simultaneously for all the M−L bonds. Here only the symmetric M−L stretching force constants were determined. An average M−L bond energy E_{ML} is defined according to

$$D_e\text{: } ML_n^{2-} \rightarrow M + (n-2)L + 2L^-, \quad E_{ML} = D_e/n \quad (8)$$

In eqs 7 and 8, the calculated ground-state atomic configurations (relativistic and nonrelativistic) are used for the transition metals. Table 5 shows that the relativistic ground-state configurations are consistent with the experimental ones and the calculated relative energies of J-averaged atomic states agree well with the experimental data. From Moore's book[44] (experimental data), the $3d^84s^2(^3F)$ and $3d^94s^1(^3D)$ states for Ni are nearly degenerate ($^3F \rightarrow {}^3D$, $\Delta E = -0.03$ eV). A relativistically corrected experimental datum[45] shows that $3d^94s^1$ lies 0.33 eV below $3d^84s^2$. We note the relativistic and nonrelativistic ground states are different for Pt.

Table 3. Calculated M−L Bond Lengths R (Å) and Force Constants k (mdyn/Å) in ML_4^{2-}

	R_{ML}^{FI}	R_{ML}^{IMP}	R_{ML}^{exp}	ΣR^{cov}	k_{ML}^{FI}	R_{ML}^{IMP}
NiH_4^{2-}	1.56 (1.57)	1.47 (1.48) 1.56[b]	1.49	1.47	1.55 (1.49)	2.73 (2.64)
PdH_4^{2-}	1.67 (1.69)	1.63 (1.65)	1.63	1.60	1.84 (1.66)	2.37 (2.21)
PtH_4^{2-}	1.69 (1.76)	1.63 (1.68)	1.62	1.62	1.87 (1.57)	2.76 (2.33)
NiH_6^{2-}	1.53 (1.54)	1.46 (1.47)			1.80 (1.73)	2.81 (2.73)
PdH_6^{2-}	1.66 (1.68)	1.62 (1.63)			2.01 (1.87)	2.42 (2.35)
PtH_6^{2-}	1.68 (1.73)	1.64 (1.68)	1.65		2.10 (1.82)	2.78 (2.41)
$NiCl_4^{2-}$	2.21 (2.22)	2.12 (2.13)		2.14	1.62 (1.56)	2.93 (2.88)
$PdCl_4^{2-}$	2.34 (2.36)	2.27 (2.29)	2.29[c]	2.27	1.71 (1.54)	2.73 (2.64)
$PtCl_4^{2-}$	2.37 (2.43)	2.30 (2.34)	2.31[c]	2.29	1.85 (1.48)	2.92 (2.62)
$NiCl_6^{2-}$	2.25 (2.26)	2.17 (2.18)			1.71 (1.67)	2.66 (2.62)
$PdCl_6^{2-}$	2.35 (2.37)	2.28 (2.30)	2.29[d]		1.86 (1.73)	2.83 (2.71)
$PtCl_6^{2-}$	2.38 (2.42)	2.31 (2.35)	2.31[d]		2.01 (1.68)	3.02 (2.71)

[a] ΣR^{cov} is the sum of Pauling's covalent radii of M and L. The values in parentheses are the nonrelativistic results. FI, free ion; IMP, ion in Madelung potential. [b] CASSCF-CI calculation by Lindberg et al.;[21] the Mdelung potential used in their calculation was determined from a charge distribution with 2− on the nickel center. [c] The original refs 6 and 4 gave $R_{PdCl}^{exp} = 2.3066$ Å and $R_{PtCl}^{exp} = 2.310(1)$ Å, but according to the atomic position parameters given there, we obtain $R_{PdCl}^{exp} = 2.2919$ Å and $R_{PtCl}^{exp} = 2.3095$ Å. [d] The situation is similar to that in *b*.

The relative stabilities of ML_6^{2-} versus ML_4^{2-} are compared in Table 6. Gross orbital populations and atomic charge distributions are given in Tables 7 and 8. In order to see the influence of the crystal field on the molecular or ionic properties, all the free complexes have also been calculated.

3.1. MH_2^{2-} and Na_2MH_2 (M = Pd, Pt). The results of free MH_2^{2-} complexes are also presented to examine the effect of the attached ligands to the M−H bonding. It is shown that

(44) Moore, C. E. *Atomic Energy Levels*; Circ. 467; U.S. GPO: Washington DC, 1959; Vols. 2 and 3.
(45) Raghavachari, K.; Trucks, G. W. *J. Chem. Phys.* **1989**, *91*, 1062.

Table 4. Calculated Bond Energies E_{ML} (eV) and Lattice Energies E_{latt} (eV) in ML_n^{2-a}

	E_{ML}^{FI}	Δ^{rel}	$E_{ML}^{internal}$	E_{latt}/m^b	E_{ML}^{IMPc}	Δ^{rel}
NiH_4^{2-}	1.97 (1.94)	0.03	2.00 (1.96)	2.60 (2.60)	4.60 (4.56)	0.04
PdH_4^{2-}	2.15 (1.87)	0.28	2.05 (1.74)	2.58 (2.57)	4.63 (4.31)	0.32
PtH_4^{2-}	2.41 (1.83)	0.58	2.46 (1.81)	2.54 (2.52)	5.00 (4.33)	0.67
NiH_6^{2-}	2.31 (2.26)	0.05	2.37 (2.32)	1.43 (1.43)	3.80 (3.75)	0.05
PdH_6^{2-}	2.35 (2.11)	0.24	2.31 (2.04)	1.46 (1.46)	3.77 (3.50)	0.27
PtH_6^{2-}	2.61 (2.10)	0.51	2.65 (2.07)	1.43 (1.42)	4.08 (3.49)	0.59
$NiCl_4^{2-}$	2.36 (2.35)	0.01	2.29 (2.27)	2.28 (2.28)	4.57 (4.55)	0.02
$PdCl_4^{2-}$	2.21 (1.99)	0.22	2.16 (1.93)	2.14 (2.13)	4.30 (4.06)	0.24
$PtCl_4^{2-}$	2.40 (1.93)	0.47	2.39 (1.82)	2.12 (2.11)	4.51 (3.93)	0.58
$NiCl_6^{2-}$	2.41 (2.39)	0.02	2.39 (2.36)	1.10 (1.10)	3.49 (3.46)	0.03
$PdCl_6^{2-}$	2.33 (2.14)	0.19	2.31 (2.12)	1.05 (1.04)	3.36 (3.16)	0.20
$PtCl_6^{2-}$	2.57 (2.14)	0.43	2.57 (2.12)	1.04 (1.03)	3.61 (3.15)	0.46

[a] The values in parentheses are the nonrelativistic results. $\Delta^{rel} = E^{rel} - E^{nrel}$. FI, free ion, IMP, ion in Madelung potential. [b] $m = 8$ for $n = 4$; $m = 12$ for $n = 6$. [c] $E_{ML}^{IMP} = E_{ML}^{internal} + E_{latt}/m$.

Table 5. Relative Energies (eV) for the Different Electronic Configurations of Ni, Pd, and Pt[a]

		$(n-1)d^8ns^2$ (^3F)	$(n-1)d^9ns^1$ (^3D)	$(n-1)d^{10}$ (^1S)
Ni	calc	0	−0.80 (−1.33)	1.44 (0.56)
	exp[b]		−0.33	1.24
Pd	calc	0	−2.54 (−3.69)	−3.30 (−5.28)
	exp[c]		−2.42	−3.43
Pt	calc	0	−0.92 (−3.56)	−0.65 (−5.34)
	exp[c]		−0.64	−0.33

[a] The values in parentheses are the nonrelativistic results. [b] After correcting or relativistic effects.[45] [c] From ref 44 and averaged over all J levels.

Table 6. Calculated Energies ΔU (eV) for Reaction $ML_6^{2-} \rightarrow ML_4^{2-} + L_2(g)$ (M = Ni, Pd, Pt; L = H, Cl). $\Delta^{rel} = \Delta U^{rel} - \Delta U^{nrel}$

	$\Delta U^{FI}(\Delta^{rel})$	$\Delta U^{IMP}(\Delta^{rel})$		$\Delta U^{FI}(\Delta^{rel})$	$\Delta U^{IMP}(\Delta^{rel})$
L = H			L = Cl		
M = Ni	1.13 (0.15)	−0.47 (0.10)	M = Ni	1.86 (0.11)	−0.48 (0.09)
M = Pd	0.71 (0.37)	−0.73 (0.38)	M = Pd	2.05 (0.31)	−0.18 (0.23)
M = Pt	1.19 (0.76)	−0.35 (0.79)	M = Pt	2.69 (0.74)	0.47 (0.42)

the presence of the ligands Na contracts the Pd−H bond by 0.06 Å. This seems counterintuitive. The explanation is that the partial transfer of electron density from the complex ion to the sodium (see population analysis in Table 7) reduces the Coulomb repulsion between the hydrogen and palladium. Upon embedding Na_2PdH_2 in the crystal field, the Pd−H bond is expanded by 0.04 Å (note that the electron densities on H and Pd are again increased by the crystal field), with the result that the calculated R_{PdH} (1.66 Å) in the MP is 0.02 Å longer than experiment (1.64 Å). However, the neutron diffraction measurement on the deuterated sample Na_2PdD_2[8] as well as the inelastic neutron scattering study[46] favors a longer Pd−H bond length (1.68 Å) and so supports our calculated Pd−H bond lengths in the MP.

The calculated H−Na bond length of free Na_2PdH_2 is remarkably underestimated (by 0.52 Å) compared to the experimental data. In the crystal field, the MP shows an overall expansion (by 0.27 Å) on H−Na. This phenomenon was also found in mercurous halides Hg_2X_2[40] and can be ascribed to the repulsion effect between the Na ion and the four nearest point charges due to their close approach (see Figure 4). In fact, the local environment of molecule Na_2MH_2 is quite similar to that of Hg_2X_2 in crystal. Still, the calculated H−Na bond length is not in very good agreement with the measured one, with a deviation of 0.25 Å. According to the atomic arrangement, there is a close approach of 3.55 Å (see Table 1) between the Na and Na atoms of neighboring molecules. So the effect of short-range overlap may be rather strong and a simple Madelung potential is unlikely to account for the strong interaction with the neighbors. In order to elucidate this factor, we have performed a second step calculation by including the eight second-nearest Na^+ ligands explicitly in the calculated system (all other ions are still approximated by point charges). It is shown that the H−Na distance calculated in such a surrounding agrees very well with the experimentally observed one.

The calculated Pt−H and H−Na bond lengths in Na_2PtH_2 are quite similar to those in Na_2PdH_2. Nonrelativistically, R_{PtH} is clearly larger than R_{PdH}. The relativistic bond contractions are 0.03 and 0.07 Å for Pd−H and Pt-H, respectively. The latter value is too small to change the bond length order.

The free MH_2^{2-} species are shown to have a relatively large bond strength (1.3−1.7 eV). By including the two ligands Na in calculation, the bond energies are increased by nearly 1 eV. In addition, the crystal field enhances the M−H bonding very strongly (by 3 eV). The lattice energy E_{latt} decreases from Na_2PdH_2 to Na_2PtH_2. Although E_{latt} on the species is relatively small, the effect of the whole crystal field has significant influence on the molecular properties. The M−H bonding in Na_2PdH_2 is slightly weaker by 0.3−0.4 eV than in Na_2PtH_2, At the nonrelativistic level, E_{PtH} is comparable to E_{PdH}. The relativistic stabilizations Δ^{rel} are significantly smaller for the free molecules than in the MP. Since M $(n-1)$ is relativistically destabilized and M ns is stabilized, the magnitude of Δ^{rel} depends on the population changes of the $(n-1)$d and ns AOs upon molecular formation. For Pd, the 5s is empty and the valence 4d shell is fully occupied. From Mulliken populations in Table 7, there is more than a 0.5 electron loss from the 4d shell. On the other hand, the gain of 5s electron contributes also to the relativistic energy increase. This is the reason why Na_2PdH_2 in the MP has larger relativistic stabilization (due to more net 5s population) than the free molecule although more d electron is lost in the free molecule than in the MP. The same is true of the Na_2PtH_2 system. In the crystalline compound, the MP greatly increases the Pt 6s population and so results in a relativistic increase in E_{PtH}.

No vibration spectra, infrared or Raman, are known for the linear molecular unit in the crystal, but an experimental Pd−H stretch force constant is available,[46] which was obtained by fitting the inelastic neutron scattering (INS) spectrum (intensity) to a harmonic force field. The calculated Pd−H force constant for the free PdH_2^{2-} complex is 0.3 mdyn/Å smaller than the INS value. The M−H force constants k_{MH} are increased by 0.5 mdyn/Å due to the presence of Na ligands. However, the M−H frequencies of the Na_2MH_2 molecules are much (more than 1500 cm^{-1}) smaller than those of free MH_2^{2-}. This is ascribed to the vibrational coupling with the adjacent Na atoms, which have a very large effect on the M−H frequency. The k_{MH} in the MP shows only a very slight increase, although there exists a large crystal field stabilization effect on the M−H bond. This is because a decrease in k_{MH} is accompanied by the bond expansion in the MP. Therefore, both the bond stabilization and expansion effects combine to determine the change of k_{MH} in the MP. The force constant k_{HNa} and frequencies ω_2 and ω_3 are affected strongly by the crystal field; i.e., they are decreased in the MP, corresponding to the H−Na bond expansion in the MP. All M−H force constants show a considerable relativistic increase, being consistent with the relativistic bond contraction. The relativistic effects on force constant k_{HNa} are substantial for Na_2PdH_2 in the MP. The calculated coupling constants k_{12} are seen to be small.

(46) Noréus, D.; Tomkinson, J. *Chem. Phys. Lett.* **1989**, *154*, 439.

Table 7. Gross Mulliken Populations on the Metal M and Atomic Charges Q on the Metal M and Ligands H and Na in MH_2^{2-} and Na_2MH_2 (M = Pd, Pt)[a]

		M $(n-1)$d	M ns	M np	Q_M	Q_H	Q_{Na}
PdH_2^{2-}	FI	9.27 (9.32)	1.79 (1.67)	0.53 (0.52)	−1.59 (−1.51)	−0.21 (−0.24)	
PtH_2^{2-}	FI	9.24 (9.36)	1.57 (1.42)	0.00 (0.00)[b]	−0.67 (−0.64)	−0.67 (−0.68)	
Na_2PdH_2	FM	9.21 (9.24)	0.18 (0.17)	0.00 (0.00)[b]	0.72 (0.67)	−0.90 (−0.91)	0.54 (0.57)
	MMP	9.44 (9.49)	0.79 (0.66)	0.02 (0.02)	−0.26 (−0.17)	−0.98 (−1.07)	1.11 (1.16)
Na_2PtH_2	FM	9.13 (9.29)	0.43 (0.50)	0.00 (0.00)[b]	0.55 (0.32)	−0.92 (−0.70)	0.64 (0.54)
	MMP	9.38 (9.48)	0.92 (0.89)	0.02 (0.03)	−0.31 (−0.40)	−0.98 (−0.96)	1.13 (1.17)

[a] The values in parentheses are the nonrelativistic results. FI, free ion; FM, free molecule; MMP, molecule in Madelung potential. [b] Negative values were obtained and so they are set as zero.

Table 8. Gross Mulliken Populations on the Metal M and Atomic Charges Q on the Metal M and Ligand L in ML_n^{2-} (M = Pd, Pt; L = H, Cl; n = 4, 6)[a]

		M $(n-1)$d	M ns	M np	Q_M	Q_L
NiH_4^{2-}	FI	8.89 (8.91)	1.06 (1.00)	0.97 (0.94)	−0.91 (−0.85)	−0.27 (−0.29)
	IMP	8.90 (8.92)	0.88 (0.86)	1.50 (1.52)	−1.28 (−1.30)	−0.18 (−0.17)
PdH_4^{2-}	FI	8.78 (8.85)	0.90 (0.71)	0.80 (0.79)	−0.48 (−0.34)	−0.38 (−0.41)
	IMP	8.94 (9.00)	0.52 (0.39)	0.33 (0.32)	0.21 (0.30)	−0.55 (−0.56)
PtH_4^{2-}	FI	8.69 (8.84)	0.90 (0.87)	0.00 (0.00)[b]	0.73 (0.69)	−0.68 (−0.67)
	IMP	8.75 (8.86)	0.43 (0.46)	0.45 (0.47)	0.37 (0.21)	−0.59 (−0.55)
$NiCl_4^{2-}$	FI	8.77 (8.80)	0.52 (0.50)	0.58 (0.59)	0.13 (0.12)	−0.53 (−0.53)
	IMP	8.78 (8.81)	0.67 (0.64)	0.74 (0.75)	−0.19 (−0.20)	−0.45 (−0.45)
$PdCl_4^{2-}$	FI	8.77 (8.89)	0.32 (0.28)	0.29 (0.31)	0.62 (0.52)	−0.66 (−0.63)
	IMP	8.79 (8.84)	0.38 (0.35)	0.25 (0.28)	0.66 (0.54)	−0.66 (−0.63)
$PtCl_4^{2-}$	FI	8.72 (8.88)	0.48 (0.33)	0.32 (0.31)	0.48 (0.48)	−0.62 (−0.62)
	IMP	8.67 (8.82)	0.54 (0.43)	0.32 (0.31)	0.47 (0.45)	−0.62 (−0.61)
$NiCl_6^{2-}$	FI	8.53 (8.56)	0.37 (0.38)	1.01 (1.02)	0.09 (0.03)	−0.35 (−0.34)
	IMP	8.55 (8.58)	0.44 (0.46)	1.68 (1.69)	−0.67 (−0.72)	−0.22 (−0.21)
$PdCl_6^{2-}$	FI	8.42 (8.56)	0.15 (0.18)	0.58 (0.61)	0.85 (0.65)	−0.47 (−0.44)
	IMP	8.53 (8.68)	0.29 (0.34)	1.00 (1.04)	0.17 (−0.06)	−0.36 (−0.32)
$PtCl_6^{2-}$	FI	8.35 (8.51)	0.23 (0.19)	0.65 (0.60)	0.77 (0.69)	−0.46 (−0.45)
	IMP	8.33 (8.49)	0.35 (0.35)	1.34 (1.29)	−0.01 (−0.13)	−0.33 (−0.31)

[a] The values in parentheses are the nonrelativistic results. FI, free ion; IMP, ion in Madelung potential. [b] Negative values were obtained and so they are set as zero.

3.2. MH_x^{2-} (M = Ni, Pd, Pt; x = 4, 6). We first discuss the complexes with $x = 4$. The calculated M−H bond lengths of the free MH_4^{2-} complexes are generally 0.07 Å longer than experimental ones. The results in the MP show clearly the bonding contracting effect of the crystal field which stabilizes the ion group (see Table 4) and counteracts the H^-−H^- repulsion. The experimental M−H bond lengths are now very well reproduced by the calculation in the MP, the error being ≤0.02 Å. The calculated and experimental Pd−H distances are shorter than those in the linear complex. This reflects the stronger bond in the square-planar d^8 complex with its lower electron density. Table 3 also gives information on Pauling's[47] covalent radii of the metals and ligands. All M−H bond lengths are very close to the sum of the covalent radii and so are indicative of covalent bonding within the complex. Therefore, two different types of bond coexist in the crystal structures: the ionic bond between the complex MH_x^{2-} and the alkali or alkaline-earth element and the covalent bond between the transition metal and the hydrogen. The relativistic bond contractions of M−H are 0.01, 0.02, and ∼0.05 Å for Ni−H, Pd−H, and Pt−H, respectively. The relativistic and nonrelativistic bond lengths follow a same monotonic order $R_{NiH} < R_{PdH} \leq R_{PtH}$. This means that the anomalous trend in bond lengths obtained for group 11 compounds[41,48] is not observed for these group 10 compounds. In contrast to the situation of Na_2MH_2, the crystal field stabilization of the MH_4^{2-} complexes is now paralleled by a significant increase of the k_{MH}'s. Due to the slightly larger MP in the Mg_2NiH_4, the increase of k is also larger. So, the order of the force constants in the MP $k_{PdH} < k_{NiH} \approx k_{PtH}$ is different from the order $k_{NiH} < k_{PdH} \approx k_{PtH}$ in vacuum.

The average M−H bond energies obtained for the free complexes are more than 2 eV, indicating that the complex ions are quite stable with respect to the atoms and ions even in vacuum. The crystal field causes only minor changes in the internal bond energy. The MP stabilizations are 2.5−2.6 eV and vary only slightly for the different complexes. The M−H bonds are relativistically stabilized, owing to the loss of electron(s) from the M $(n-1)$d shell (see Table 8) upon complex formation. The losses of the $(n-1)$d electron(s) are 0.1, 1.1−1.2, and 0.2−0.3 for Ni, Pd, and Pt, respectively. The value of Pd is nearly one electron more than that of Pt (because of the different ground atomic configurations). Therefore the relativistic stabilization of the Pd−H bond is also found to be significant. This happens also for the chlorides (see section 3.3). Because of the small atomic number of Ni, the relativistic effects are also expected to be small. The bond strengths follow the stability sequence $E_{NiH} < E_{PdH} < E_{PtH}$ for the free complexes and $E_{NiH} \approx E_{PdH} < E_{PtH}$ in the MP. The relativistic effects are responsible for the orders. These trends are in agreement with the experimental fact that PtH_4^{2-} is the most common within the group 10 A_2MH_4 compounds.

We now compare the calculated properties of MH_6^{2-} with those of MH_4^{2-}. The M−H bond lengths in MH_6^{2-} are very similar to those in MH_4^{2-}, in agreement with the neutron diffraction measurements on K_2PtH_4[16] and K_2PtH_6.[25] The relativistic bond contractions in MH_6^{2-} and MH_4^{2-} are also very similar. The force constant in MH_6^{2-} is about 0.1−0.2 mdyn/Å larger than in MH_4^{2-}. This also leads to a 0.2−0.3 eV increase in the (internal) bond energy. However, the lattice energy

(47) Pauling, L. *Z. Kristallogr*. **1928**, *80*, 377.
(48) Schwerdtfeger, P.; Dolg, M.; Schwarz, W. H. E.; Bowmaker, G. A.; Boyd, P. D. *J. Chem. Phys*. **1989**, *91*, 1762.

Table 9. Calculated ionization potentials (eV) of Ni, Pd, and Pt[a]

		1.IP[b]	2.IP[b]	3.IP[b]	4.IP[b]
Ni	Calc	7.93 (7.67)	19.35 (19.51)	35.37 (35.70)	54.44 (54.95)
	exp[c]	7.635	18.168	35.17	54.9
Pd	calc	8.53 (8.67)	19.84 (20.16)	33.07 (33.54)	47.49 (48.09)
	exp[c]	8.34	19.43	32.93	
Pt	calc	8.73 (7.24)	19.15 (19.66)	31.03 (31.76)	44.18 (45.03)
	exp[c]	9.0	18.563		

[a] The values in parentheses are the nonrelativistic results. [b] Electronic configurations used in calculating the IPs are Ni^0, $3d^94s^1$, Pd^0, $4d^{10}$; Pt^0, $5d^96s^1$; Ni^+, $3d^9$, Pd^+, $4d^9$; Pt^+, $5d^9$; Ni^{2+}, $3d^8$; Pd^{2+}, $4d^8$; Pt^{2+}, $5d^8$; Ni^{3+}, $3d^7$; Pd^{3+}, $4d^7$; Pt^{3+}, $5d^7$. [c] Reference 44.

contribution to the M−H bond, E_{latt}/m, is considerably different in MH_6^{2-} than in MH_4^{2-}. E_{latt}/m in MH_6^{2-} is 1.1−1.2 eV smaller than that in MH_4^{2-}. The difference $\Delta^{II-IV} E_{latt}$ in the lattice energies between MH_4^{2-} and MH_6^{2-} is just the cause for the relative instability of MH_6^{2-} to MH_4^{2-} in the solid state (see section 3.4).

3.3. MCl_y^{2-} (M = Ni, Pd, Pt; y = 4, 6). For the free complexes, the calculated M−Cl bond lengths exceed the experimental ones by 0.05−0.07 Å. Also in the MP, the calculated Pd−Cl and Pt−Cl distances are very close to the values obtained from the X-ray determinations. The calculated difference, $R_{PtCl} - R_{PdCl}$, of 0.03 Å agrees with the experimental observation (0.02 Å). According to the X-ray measurements, the M−Cl bond lengths for M = Pd, Pt do not vary from K_2MCl_4 to K_2MCl_6. The calculation shows also that the M−Cl bond lengths in MCl_4^{2-} and MCl_6^{2-} are almost identical. Comparable experimental Ni−Cl bond lengths for square $NiCl_4^{2-}$ and octahedral $NiCl_6^{2-}$ are not available. Tetrahedral $NiCl_4^{2-}$ moieties in crystal compounds[49] have a Ni−Cl distance of ∼2.26 Å. This value is 0.14 Å larger than the calculated one in square complex. A calculation on free tetrahedral $NiCl_4^{2-}$ (unpublished results) shows a Ni−Cl distance of 2.30 Å which is ∼0.1 Å larger than that in free square $NiCl_4^{2-}$. In contrast to NiH_x^{2-} [$R(x = 6) - R(x = 4) = -0.03$ Å], the Ni−Cl bond length in $NiCl_6^{2-}$ is now 0.03−0.04 Å longer than in $NiCl_4^{2-}$. It seems that the activation of the nonbonding d_{z^2} orbital in ML_4^{2-} by addition of two more L ligands does not change the Pd−L and Pt−L bond lengths, but this is not true for the Ni complex. The relativistic bond contractions are also small in these complexes and comparable to those in the hydrides. The force constants of MCl_4^{2-} and MCl_6^{2-} are not substantially different.

The average M−L bond strength in MCl_n^{2-} is comparable to that in MH_n^{2-} for M = Pd, Pt. The difference is relatively larger for M = Ni. The lattice energy on M−L is 0.3−0.5 eV smaller in MCl_n^{2-} than in MH_n^{2-}. The chlorides MCl_4^{2-} follow the bond strength sequence $E_{PdCl} < E_{NiCl} \approx E_{PtCl}$. The main difference between MCl_6^{2-} and MCl_4^{2-} is also the lattice energy contribution to the M−Cl bond; i.e., the lattice energy on M−L is significantly larger in MCl_4^{2-} than in MCl_6^{2-}. By summing up the lattice energies on whole bonds, $\Delta^{II-IV}E_{latt}$ for L = Cl is even larger than that for L = H. Nevertheless, the next section will show the fact that the MCl_6^{2-} complex is stable relative to MCl_4^{2-} with M = Pd and Pt.

3.4. Relative Stability of ML_6^{2-} versus ML_4^{2-}. The Pd and Pt elements form compounds in which they can be di- and tetravalent, respectively. In contrast, the oxidation state of Ni is mainly restricted to II. This fact may be roughly explained by the ionization potentials (IP) $M^+ \rightarrow M^{2+}$ and $M^{3+} \rightarrow M^{4+}$. Table 9 shows that the fourth IPs in Pd and Pt are significantly smaller than in Ni (note that the calculated IPs agree reasonably with available experimental data[44], although the frozen core approximation has been applied). This simply reflects the difference in stability of the higher oxidation state among the group 10 elements. However, as pointed out,[50] oxidation numbers in chemical compounds do not correspond to measurable quantities. It is apparent that Pd and Pt show much less tendency to attain the higher oxidation state IV in hydrides than in halides. The strong dependence of the higher oxidation state on the nature of ligand needs to be explained.

According to Table 4, for a given metal M and ligand L, the average bond energies E_{ML} of free ML_6^{2-} and ML_4^{2-} are substantially the same, and in the MP the order $E_{ML}(ML_6^{2-}) < E_{ML}(ML_4^{2-})$ always holds. The trends in the bond strengths are similar with the different M and different L. Therefore, the relative size of the bond energies cannot account for the relative stability, although there is a correlation between the bond strength and the compound stability. The following reaction allows the relative thermodynamic stability of ML_6^{2-} versus ML_4^{2-} to be evaluated.

$$ML_6^{2-} \rightarrow ML_4^{2-} + L_2(g) \qquad (9)$$

The elimination reaction forms one L−L bond at the expense of two M−L bonds.

The reaction energies are given in Table 6. For the free complex, the disproportionation reaction 9 is rather endothermic with both L = H and Cl, indicating that ML_6^{2-} is stable relative to ML_4^{2-}. The disproportionation of the MH_6^{2-} ion is seen to be much more favorable than that of MCl_6^{2-} although the average M−L bond strength in MH_n^{2-} is similar to that in MCl_n^{2-}. This is because the differential stability of the elimination product $L_2(g)$ strongly affect the reaction energy, the elimination of more weakly bound Cl_2 ($D_e^{exp} = 2.52$ eV[51], $D_e^{calc} = 3.14$ eV) being much less favorable than that of H_2 ($D_e^{exp} = 4.75$ eV[51], $D_e^{calc} = 4.83$ eV).

The results obtained in the MP clearly show the crystal field destabilization effect on the higher oxidation state in M. Equilibrium 9 is strongly shifted to the right by the crystal field effect. It is exothermic by 0.35−0.73 eV with L = H; i.e., the MH_6^{2-} complexes are less stable than the MH_4^{2-} ones. However, PtH_6^{2-} is the least unstable complex and the disproportionation energy (∼34 kJ/mol) is seen not to be so pronounced. This may be the reason why it has been possible to obtain the A_2PtH_6 compounds under special conditions (i.e., very high pressures of hydrogen). On the other hand, the evidence for the instability of PtH_6^{2-} relative to PtH_4^{2-} is the fact that K_2PtH_6 can be converted into $K_2PtH_4 + H_2$ at a temperature above 500 K.[25] In contrast, a preparation of A_2PdH_6 compounds would become much more difficult according to the calculated reaction energy for M = Pd. It is now understood that hydrides have not been accessible that contain palladium in the same oxidation state IV as those containing platinum. The calculated order of stability, $PdH_6^{2-} < NiH_6^{2-} < PtH_6^{2-}$ suggests that the preference for higher oxidation state in hydrides should be least pronounced for Pd among group 10 elements. The order of the ΔU values is in agreement with the overall increase in the average M−H bond energies.

With L = Cl, the elimination reaction for M = Ni is rather exothermic. So $NiCl_6^{2-}$ in the crystal field is unstable and will

(49) (a) Pauling, P. *Inorg. Chem.* **1966**, *5*, 1498. (b) Weisner, J. R.; Srivastava, R. C.; Kennard, C. H. L.; Di Vaira, M.; Lingafelter, E. C. *Acta Crystallogr.* **1967**, *23*, 565.

(50) Schwerdtfeger, P.; Boyd, P. D. W.; Brienne, S.; Burrell, A. K. *Inorg. Chem.* **1992**, *31*, 3411.

(51) Huber, K. P.; Herzberg, G. *Molecular Spectra and Molecular Structure, Vol. IV, Constants of Diatomic Molecules*; Van Nostrand Reinhold: New York, 1979.

decomposes into $NiCl_4^{2-} + Cl_2(g)$. The ΔU value for M = Pd is slightly negative. The relatively small value of ΔU indicates that palladium(IV) and palladium(II) chlorides have a comparable stability. From M = Pd to M = Pt, the reaction energy even changes from exothermic to endothermic. All these results are in accordance with the experimental evidence that both $PdCl_6^{2-}$ and $PtCl_6^{2-}$ exist but $NiCl_6^{2-}$ does not. In contrast to the hydrides, the chlorides exhibit a monotonic order of stability $NiCl_6^{2-} < PdCl_6^{2-} < PtCl_6^{2-}$. This order is also inconsistent with the order in the average bond energies along this series.

Without considering the bond energies of the elimination products L_2, all ML_6^{2-} complexes are still much more stable than the corresponding ML_4^{2-} ones. Therefore, the stability of L_2 is decisive for the relative stability of M(IV) versus M(II). In this case, it is the rather high stability of H_2 that is responsible for the relative instability of M(IV) in the hydrides.

The relativistic bond strengthening in ML_6^{2-} for a whole complex is more pronounced than that in ML_4^{2-}. Therefore, the stability balance of M(IV) versus M(II) is shifted in favor of M(IV) by the relativistic effects. The relativistic stabilization can be attributed to the notably smaller M $(n-1)$d population in the M(IV) complex than in M(II) one (see Table 8). $\Delta^{rel}\Delta U$ values for the hydrides are large. They are 0.1, 0.4, and 0.8 eV for M = Ni, Pd, and Pt, respectively, independent of the complex state (free ion or in MP). The relativistic increase of Δ^{rel} (0.8−0.4 = 0.4 eV) from Pt to Pd is comparable to the total energy difference in the MP (0.41 eV). Therefore, most of the difference in stabilities of PdH_6^{2-} and PtH_6^{2-} can be attributed to the relativistic effects. For the chlorides, $\Delta^{rel}\Delta U$ is larger for the "soft" ion (0.1, 0.3, and 0.7 for M = Ni, Pd, and Pt, respectively) than for the restraining crystal field (0.1, 0.2, and 0.4 for M = Ni, Pd, and Pt, respectively), and the total energy difference between Pd and Pt in the MP (0.65 eV) is remarkably larger than the relativistic increase (0.2 eV). So the relativistic effects are not a dominant factor in the stability difference between the palladium(IV) and platinum(IV) chlorides. The strong dependence of relativistic effects on the choice of ligand was also found in the Au(I) and Au(III) complexes.[52] The nonrelativistic ΔU value for M = Pd and L = Cl is −0.41 eV, showing a significant instability of $PdCl_6^{2-}$. So the existence of $PdCl_6^{2-}$ may be the relativistic effects. Although relativistic effects contributes substantially to the stability of $PtCl_6^{2-}$, they may not be the main reason for the high valency of Pt because the nonrelativistic ΔU value for M = Pt has already been positive.

3.5. Mulliken Population Analysis. Table 7 shows the gross Mulliken populations and atomic charges MH_2^{2-} and Na_2MH_2 (M = Pd, Pt). In order to examine relativistic effects on these properties, the quasi-relativistic approach[53] has been used to produce the relativistic results (in which spin−orbit coupling is excluded). The M d populations are all more than 9. Except for PdH_2^{2-}, the M *n*p orbitals participate very weakly in the occupied MOs. In free MH_2^{2-}, there is a large electron transfer from H^- to M, especially for PdH_2^{2-}. The presence of Na ligands strongly reduces the atomic charge of M and increases the atomic charge of H (we specify that the atomic charge is larger when it is more negative). On the other hand, the ionicity of the H−Na bond is reinforced by the crystal field. The calculated atomic charges on H and Na are nearly 1− and 1+, respectively, which justify the charges that have been used to calculate the MP.

The Mulliken populations of the ML_n^{2-} complexes are given in Table 8. the M $(n-1)$d population is about 8.3−9.0 and hardly influenced by the crystal field. There is a smaller d population in the Pt(IV) compounds than in the Pd(IV) ones, which reflects the fact that the higher *n*IPs ($n > 1$) are smaller for Pt than for Pd. The M *n*p orbitals now participate considerably in the occupied MOs (the exceptions are free PtH_4^{2-} and PdH_4^{2-} in the MP). For the hydrides, the M *n*s population is greatly decreased by the crystal field, but this is opposite for the chlorides. The positive atomic charges Q_M on the metals are all less than 1+. In some cases, Q_M values are even negative. Therefore the complexes are mainly described by a strong covalent M−L bonding, as indicated by the rather short calculated bond lengths. For the MH_4^{2-} and MCl_6^{2-} systems, the crystal field raises the atomic charges on M and so enhances the covalency between M and L. The atomic charge Q_{Cl} in $NiCl_4^{2-}$ is larger than Q_H in NiH_4^{2-}, corresponding to the order of ligand electronegativity. Because of the fact that Cl is a better π donor than H, the opposite case also occurs usually. The atomic charges decrease along the order $Q_{Pd} < Q_{Pt} < Q_{Ni}$. The relativistic effects generally decrease the atomic charge on the M, but in most cases, the relativistic effects on the charge distributions are small.

4. Summary

A theoretical study of the complexes MH_x^{2-} and MCl_y^{2-} in the crystalline A_2MH_x and A_2MCl_y compounds (A = alkali, alkaline earth; M = Ni, Pd, Pt; $x = 2, 4, 6$; $y = 4, 6$) has been carried out using relativistic density-functional method. The effects from the surrounding crystal are simulated by a cutoff-type Madelung potential of point charges at the lattice sites. Bond lengths, bond energies, and force constants or vibrational frequencies are determined. The relative stability of ML_6^{2-} versus ML_4^{2-} in both vacuum and the crystal field is assessed by the elimination reaction of eq 9. A summary is given as follows:

(1) The use of a cutoff-type Madelung potential for the crystalline environments is adequate and leads to bond lengths in very good agreement with those from the neutron and X-ray diffraction measurements.

(2) The free MH_2^{2-} and MH_4^{2-} complexes are calculated to be quite stable with respect to the fragments, and their energy potential surfaces have (local) minima. This is contrary to the argument[1] that the isolated MH_x^{n-} groups are only expected to be stabilized in a matrix of cations.

(3) The linear Na_2PdH_2 moiety in the solid differs significantly from the free Na_2PdH_2 molecule and even so from the free PdH_2^{2-}. The PdH_2^{2-} unit is strongly influenced by the nearest two Na ligands and the crystal field. The long-range electrostatic potential and the short-range repulsion between Na^+ and its trans neighboring Na^+ ions are responsible for the especially long H−Na bond length in the Na_2PdH_2 compound. The crystal field contracts the M−L bond length in the ML_n^{2-} ($n = 4, 6$) complex by 0.05−0.09 Å and strongly increases the corresponding force constant (by ∼1 mdyn/Å). The M−L bond lengths are nearly equal in the M(II) and M(IV) complexes. The relativistic bond contractions of M−L are small and do not cause anomalies within the group 10 series of compounds. This is in contrast to group 11-containing compounds.[41,48] The explanation for the rather small $\Delta^{rel}R_{ML}$ for the Pd and Pt compounds relative to those in many Ag(I) and Au(I) species may lie in a very large M $(n-1)$d participation in the M−L bond for M = Pd, Pt. This participation would quench the bond contraction caused by the relativistic *n*s contraction.

(4) The crystal field effect strongly shifts the equilibrium 9 to the right and contributes strongly to the destabilization of

(52) Schwerdtfeger, P. *J. Am. Chem. Soc.* **1989**, *111*, 7261.
(53) Ziegler, T.; Tschinke, V.; Baerends, E. J.; Snijders, J. G.; Ravenek, W. *J. Phys. Chem.* **1989**, *93*, 3050.

higher valency in the metal elements. However, the stability or instability of ML_6^{2-} depends also on the bond strength of the elimination product L_2. Therefore, the greater instability of M(IV) relative to M(II) in the hydrides can be attributed to a combination of solid-state effect and the high stability of the gas product H_2. However, the calculated reaction energy of eq 9 for M = Pt may not be thought in contradiction with the experimental facts.

(5) There is monotonic upward trend in the reaction energies of eq 9 for the chlorides, indicating an increase in stability of the higher oxidation state from Ni to Pt. This is in contrast to the behavior of the group 13, 14, or 15 elements which show a decrease in stability of higher state with row number.[54] $NiCl_6^{2-}$ is predicted to be unstable in solid state. Thus, Ni predominantly has lower oxidation state of II, in agreement with experimental observation. The stability order $PdCl_6^{2-} < PtCl_6^{2-}$ agrees also with the known fact that Pd(IV) compounds are generally less stable than those of Pt(IV).[55]

(6) The relativistic contribution favors formation of ML_6^{2-} and increases from M = Ni to Pt and from Cl to H. The stability difference between palladium(IV) and platinum(IV) hydrides could be attributed to the relativistic effects.

(7) The study of the MH_x^{2-} complexes in the K_2MH_x (M = Pd, Pt; x = 4 or 6) systems gives valuable insight into understanding the bonding properties of the complexes in the isostructural A_2MH_x systems (A = Na, Rb, Cs).

Acknowledgment. We are grateful to Dr. W.-Z. Weng for his assitance in the preparation of the figures. Thanks go also to the reviewers for their constructive comments. This work was supported by the China Postdoctoral Science Foundation and the State Educational Commission of China.

IC960369I

(54) Schwerdtfeger, P.; Heath, G. A.; Dolg, M.; Bennett, M. A. *J. Am. Chem. Soc.* **1992**, *114*, 7518.
(55) Cotton, F. A.; Wilkinson, G. *Advanced Inorganic Chemistry*, 4th Ed.; John Wiley & Sons, Inc.: New York, 1980.